Journal of Energy Chemistry xxx (2017) xxx–xxx

Contents lists available at ScienceDirect

Journal of Energy Chemistry

journal homepage: www.elsevier.com/locate/jechem

http://www.journals.elsevier.com/journal-of-energy-chemistry/

Effect of rubrene:P3HT bilayer on photovoltaic performance of perovskite solar cells with electrodeposited ZnO nanorods

Q1 Christian Mark Pelicano*, Hisao Yanagi

Q2 *Graduate School of Materials Science, Nara Institute of Science and Technology, 8916-5 Takayama, Ikoma, Nara 630-0192, Japan*

ARTICLE INFO

Article history:
Received 23 September 2017
Revised 21 November 2017
Accepted 21 November 2017
Available online xxx

Keywords:
Rubrene:P3HT bilayer
Electrodeposited ZnO nanorods
Perovskite solar cells

ABSTRACT

Improved photovoltaic performance of perovskite solar cells is demonstrated through the synergistic effect of electrodeposited ZnO nanorods and rubrene:P3HT bilayer as electron and hole-transporting layers, respectively. Highly crystalline ZnO nanorods were obtained by electrochemical deposition in a chloride medium. Additionally, rubrene interlayer was able to passivate or cover the grain boundaries of perovskite film effectively that led to reduced leakage current. A perovskite solar cell optimized with ZnO nanorods and rubrene:P3HT bilayer achieved a maximum efficiency of 4.9% showing reduced hysteresis behavior compared with the device having P3HT as the only hole-transporting layer. The application of longer nanorods led to better perovskite infiltration and shorter charge carrier path length. These results highlight the potential of electrodeposited ZnO nanorods and rubrene:P3HT bilayer as charge selective layers for efficient perovskite solar cells.

1. Introduction

Organic–inorganic metal halide perovskite compounds have recently drawn tremendous research attention for their potential application in optoelectronics, specifically in the field of photovoltaics. In less than a decade of research, perovskite solar cells have demonstrated a remarkable increase in power conversion efficiency (PCE) that exceeded 22% through crystal growth control and interface engineering [1, 2]. These superior recorded efficiencies can be mainly associated with the unique chemical and physical properties of lead-halide perovskite materials including high light absorption coefficient [3], high charge carrier mobilities [4], small excitonic binding energy [5], long charge diffusion length [6], and tunable band gap [7]. In addition, this type of solar cells can be fabricated at low temperature by simple solution processing which makes it suitable for large-scale production. Most highly efficient perovskite solar cells employ nanostructured or mesoporous TiO_2 scaffold as the electron selective layer [8,9]. The main reasons for the utilization of TiO_2 are good band alignment with the perovskite materials, wide band gap of 3.2 eV and excellent hole blocking capability due to its deep valence band position [10,11]. However, the low electron mobility of TiO_2 triggers insufficient charge separation at the electron-transporting layer and perovskite interface [12]. High temperature sintering in the range of 450−550°C is also necessary to synthesize such complex TiO_2 structures, which render them incompatible for production of flexible solar cell devices [13]. Therefore, it is necessary to explore new alternative materials and structures that are appropriate for high performance flexible solar cells. In this respect, ZnO seems to be a potential replacement having a similar wide band gap of 3.37 eV suitable for transparent electron transport layer and higher electron mobility than TiO_2 [14,15]. High quality ZnO nanostructures can also be fabricated at low temperatures using various solution techniques [16–20]. Balela et al. have reported a highly efficient perovskite solar cell with a PCE of 15.7% based on ZnO nanoparticles prepared by spin coating [20]. Another study demonstrated that high aspect ratio N-doped ZnO nanorods produced by hydrothermal method could be utilized as electron-transporting layer in perovskite solar cells, which resulted in a PCE of 16.1% [21]. On the other hand, several materials have been designed as candidates for hole-transporting layer in perovskite solar cells such as NiO, CuSCN [22,23], polymers (P3HT, PEDOT:PSS) [24,25], and small molecules (Spiro-MeOTAD, TPB) [26,27]. Most efficient perovskite solar cells are based on Spiro-MeOTAD owing to its matched energy level alignment with perovskite interface, minimizing the energy loss from charge carrier recombination [28,29]. However, the complex and costly production of Spiro-MeOTAD, as well as, its instability in the presence of additives have driven researchers to explore more stable, cheaper but viable hole-transporting materials [30].

Herein, ZnO nanorods were grown by electrochemical deposition in a chloride medium. This technique is very attractive for solar cell application due to its low temperature operation, simplicity,

Q3 * Corresponding author.
E-mail address: christian.pelicano.ce0@ms.naist.jp (C.M. Pelicano).

https://doi.org/10.1016/j.jechem.2017.11.018
2095-4956/

cost-effectiveness and potential for large-scale production. Moreover, we introduced rubrene in a regular type perovskite solar cell as an interlayer between $CH_3NH_3PbI_3$ and P3HT films. Rubrene is a classical p-type organic semiconductor with high hole mobility and chemical stability. It has been widely used in organic light emitting diodes and thin film transistors [31,32]. In this study, we adopted the rubrene interlayer for the first time in a perovskite solar cell based on electrodeposited ZnO nanorods.

2. Experimental

2.1. Electrochemical deposition of ZnO nanorods

The indium tin oxide (ITO)-coated glass substrates (15 Ω sq^{-1}, Luminescence tech. Corp.) were cleaned through sequential ultrasonic treatments with detergent, ultrapure water, acetone and methanol for 15 min each. Prior to electrodeposition, a 0.25 M zinc acetate ($Zn(CH_3COO)_2$, Wako) in methanol:water (10:1) solution was spin-coated onto UV–O_3-treated ITO-glass substrate at 1500 rpm for 30 s. After drying at 100°C for 15 min, the films were then annealed at 350°C for 20 min to form ZnO compact layer [34].

A three-electrode electrochemical configuration was employed for the synthesis of ZnO nanorods [35]. The seeded ITO-glass substrate acted as the working electrode, a zinc wire operated as the counter electrode, and saturated calomel electrode (SCE) worked as the reference electrode. The substrates were fixed to a rotating electrode with a constant rotation speed of 100 rotations per minute (rpm). The deposition bath was maintained at 70°C containing 0.05 M KCl (99.5%, Nacalai Tesque) and 5 mM $ZnCl_2$ (98%, Nacalai Tesque). The electrolyte was saturated with pure O_2 by bubbling through a glass frit before and during the growth process. The effective area of the electrodeposited surface was about 1.54 cm^2. Electrodeposition was performed at a constant applied voltage of −1.0 V/SCE for 10–20 min using a Hokuto Denko HSV-110 potentiostat. After deposition, the samples were immediately rinsed with deionized water and annealed at 350°C for 1 h. Finally, the samples were transferred to a nitrogen-filled glove box for perovskite deposition.

2.2. Fabrication of perovskite solar cells

The $CH_3NH_3PbI_3$ layer was deposited on top of ZnO nanostructures using fast deposition crystallization as reported in the literature [36]. The perovskite precursor solution (45 wt%) was prepared by mixing 1:1 mol ratio of PbI_2 (99.999%, Wako) and CH_3NH_3I (98.0%, Wako), respectively, in 1 mL of anhydrous N,N-dimethylformamide (DMF, Wako). Then, a 60 µL of this perovskite precursor solution was spin coated on top of electrodeposited ZnO nanorods for 30 s. The substrates were spun at 5000 rpm and after 8 s, 50 µL of toluene was quickly dropped onto the center of the substrate and followed by thermal annealing at 70°C for 10 min. After cooling at room temperature, 60 µL of rubrene in toluene solution (5 mg mL^{-1}) was spin-coated on top of the perovskite layer and the films were placed in a vacuum chamber for 15 min. Subsequently, P3HT (Sigma Aldrich) in chlorobenzene solution (15 mg mL^{-1}, Wako) was spin-coated at 1500 rpm for 120 s.For complete drying of P3HT layer, the samples were then stored in nitrogen-filled glove box for 12 h in dark. Finally, 50 nm Ag electrodes were deposited by thermal evaporation under a base pressure of 2×10^{-4} Pa. The active area of the devices is 0.09 cm^2. The solar cell devices were completed by putting silver paste in the electrode areas and stored again in vacuum to dry up before measurements.

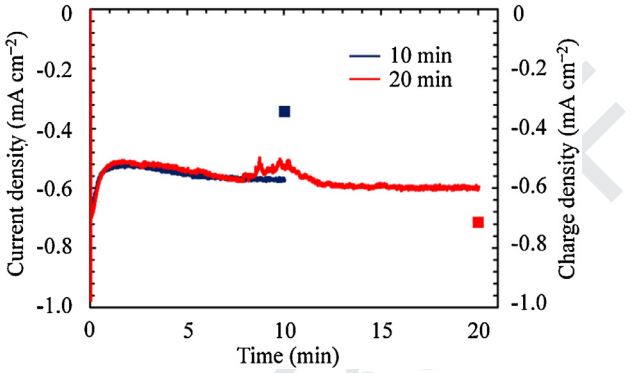

Fig. 1. Variation of current density (lines) as a function of electrodeposition time and total electrical charge density exchanged (square dots) for two deposition potentials.

2.3. Solar cell and materials characterization

The top-view and cross-sectional images were taken by a low-vacuum scanning electron microscope (SEM, Hitachi SU6600). The focused ion beam-assisted (Hitachi FB2200) cross-sectional SEM image and elemental EDX mapping analysis were obtained through ultra-high-resolution field emission scanning electron microscope (UHR FE-SEM, Hitachi SU9900). Atomic force microscopy (AFM) images were taken using a scanning probe microscope (Seiko SPA-400). Raman scattering measurement was performed at room temperature using a JASCO NRS-4100 Raman Spectrometer. The XRD patterns were characterized by a Rigaku X-ray diffractometer (RINT-TTR III) with CuK_α radiation ($\lambda = 1.542$ Å). The optical transmission and absorption spectra of the films were obtained on a UV–vis spectrophotometer (JASCO V-530). Photoluminescence spectra were measured under ultraviolet excitation ($\lambda_{ex} = 365$ nm) using a high-pressure mercury-vapour light source (Olympus BH2-RFL-T3) coupled with a microscope (Olympus BX51) and a CCD spectrometer (Hamamatsu PMA-12). Current-voltage (*J-V*) curves were recorded from a Keithley 2611B System Source Meter unit under AM 1.5 G illumination (100 mW cm^{-2}, Bunko–Keiki, CEP-2000RP). The external quantum efficiency (EQE) spectra were obtained under illumination of monochromatic light using the same system at an intensity of 1.25 mW cm^{-2}.

3. Results and discussion

First, a compact layer of ZnO nanocrystals with a mean thickness of 30 nm was deposited by spin coating on cleaned indium tin oxide (ITO)-coated glass substrates. These nanocrystals serve as a compact hole-blocking layer and at the same time as nucleation sites for nanorod growth. The ZnO nanorods for electron extraction were grown on the seeded substrates by electrochemical deposition for 10–20 min using 0.05 M KCl and 5 mM $ZnCl_2$ with an applied potential of −1.0 V vs. SCE at a temperature of 70°C. Through application of a cathodic potential, OH^- ions (Eq. 1) are electrochemically generated which increases the local pH near the seed layer-ITO electrode surface. At the same time, these OH^- ions react with Zn^{2+} ions, which eventually result in the precipitation of ZnO crystals, as shown in Eq. (2):

$$O_{2(g)} + 2H_2O_{(l)} + 4e^- \rightarrow 4OH^- \quad (1)$$

$$Zn^{2+}_{(aq)} + 2OH^-_{(aq)} \rightarrow ZnO + H_2O \quad (2)$$

Fig. 1 represents the variation of current density with time of the electrodeposited ZnO nanorods. The curves have similar features observed from the electrodeposition of ZnO using nitrate and

Please cite this article as: C.M. Pelicano, H. Yanagi, Effect of rubrene:P3HT bilayer on photovoltaic performance of perovskite solar cells with electrodeposited ZnO nanorods, Journal of Energy Chemistry (2017), https://doi.org/10.1016/j.jechem.2017.11.018